Journal of Cell Science 111, 3347-3356 (1998)
Printed in Great Britain © The Company of Biologists Limited 1998
JCS9825

Synaptojanin family members are implicated in endocytic membrane traffic in yeast

Birgit Singer-Krüger*, Yasuo Nemoto, Laurie Daniell, Susan Ferro-Novick and Pietro De Camilli‡

Howard Hughes Medical Institute and Department of Cell Biology, Yale University School of Medicine, 295 Congress Ave., New Haven CT, 06510, USA

*Present address: University of Stuttgart, Germany

‡Author for correspondence (e-mail: pietro.decamilli@yale.edu)

Accepted 18 September; published on WWW 28 October 1998

SUMMARY

The synaptojanins represent a subfamily of inositol 5′-phosphatases that contain an NH_2-terminal Sac1p homology domain. A nerve terminal-enriched synaptojanin, synaptojanin 1, was previously proposed to participate in the endocytosis of synaptic vesicles and actin function. The genome of *Saccharomyces cerevisiae* contains three synaptojanin-like genes (*SJL1*, *SJL2* and *SJL3*), none of which is essential for growth. We report here that a yeast mutant lacking *SJL1* and *SJL2* (Δ*sjl1* Δ*sjl2*) exhibits a severe defect in receptor-mediated and fluid-phase endocytosis. A less severe endocytic defect is present in a Δ*sjl2* Δ*sjl3* mutant, while endocytosis is normal in a Δ*sjl1* Δ*sjl3* mutant. None of the mutants are impaired in invertase secretion. The severity of the endocytic impairment of the *sjl* double mutants correlates with the severity of actin and polarity defects. Furthermore, the deletion of *SJL1* suppresses the temperature-sensitive growth defect of *sac6*, a mutant in yeast fimbrin, supporting a role for synaptojanin family members in actin function. These findings provide a first direct evidence for a role of synaptojanin family members in endocytosis and provide further evidence for a close link between endocytosis and actin function.

Key words: Dynamin, Clathrin, Inositol 5′-phosphatase, Actin, Mitochondria

INTRODUCTION

Inositol 5′-phosphatases represent a family of proteins which cleave the phosphate on the 5′ position of the inositol ring of inositol polyphosphates and/or phosphoinositides (Jefferson et al., 1997; Woscholski and Parker, 1997; Mitchell et al., 1996). In agreement with the multiple functions of inositol metabolites in cell physiology (De Camilli et al., 1996; Toker and Cantley, 1997; Berridge, 1997), members of this protein family have been implicated in a variety of cellular processes ranging from intracellular signaling, cytoskeletal function and membrane dynamics including vesicular traffic (reviewed by Woscholski and Parker, 1997; Mitchell et al., 1996).

A subset of inositol 5′-phosphatases, referred to as synaptojanins (McPherson et al., 1994b; McPherson et al., 1996; Nemoto et al., 1997; Srinivasan et al., 1997), are characterized by a three-domain structure. In these enzymes the central catalytic domain is flanked by a variable COOH-terminal region that is rich in prolines and an NH_2-terminal domain with homology to the cytoplasmic domain of the yeast protein Sac1p. This protein is implicated in the control of phosphatidylinositol (PtdIns) metabolism (Kearns et al., 1997), and *sac1* mutant alleles were independently identified as suppressors of mutations in the actin gene (sac = suppressor of actin) and in the gene encoding the yeast phosphatidylinositol transfer protein Sec14p (Novick et al., 1989; Cleves et al., 1989; Whitters et al., 1993).

The variable COOH-terminal domains of the synaptojanins contain multiple protein-protein interaction modules. One of their putative functions is to target specific synaptojanin family members to distinct subcellular sites (McPherson et al., 1996; Nemoto et al., 1997; Haffner et al., 1997; Cremona and De Camilli, 1997). Synaptojanin 1, which is highly enriched in nerve terminals (McPherson et al., 1996), was proposed to play a key role in the clathrin-dependent endocytosis of synaptic vesicles (McPherson et al., 1994a,b; Haffner et al., 1997). In addition, it has been implicated in the function of the actin cytoskeleton and in intracellular signaling (Mitchell et al., 1996; Sakisaka et al., 1997). Interacting partners for its alternatively spliced COOH-terminal region include proteins with a role in endocytosis and/or signaling such as amphiphysin (David et al., 1996; McPherson et al., 1996; Bauerfeind et al., 1997; Wigge et al., 1997; de Heuvel et al., 1997; Micheva et al., 1997), Eps15 (Haffner et al., 1997), the adaptor protein Grb2 (McPherson et al., 1994b; Sakisaka et al., 1997) and the SH3p4/SH3p8/SH3p13 protein family (endophilin family) (Ringstad et al., 1997; de Heuvel et al., 1997). Synaptojanin 2 is very similar to synaptojanin 1 in the Sac1p and catalytic domains, but differs in the COOH-terminal domain (Nemoto et al., 1997; Khvotchev and Südhof, 1998).

Sequencing of the genome of *Saccharomyces cerevisiae* has demonstrated the existence of four proteins with the signature motif of inositol 5′-phosphatases (Goffeau et al., 1997). Three

Table 1. Strains of *S. cerevisiae* used in this study

Yeast strain	Genotype	Source
RH2878	*Mat***a** *his3 ura3 leu2 lys2 ade2 bar1-1*	H. Riezman, Basel
NY1210	*Mat***a** *his3 ura3 leu2 gal2*$^+$	P. Novick, New Haven
NY1211	*Matα his3 ura3 leu2 gal2*$^+$	P. Novick, New Haven
BS64	*Mat***a** *his4 ura3 leu2 lys2 bar1-1*	Singer-Krüger et al. (1994)
BS188	*Matα his4 ura3 leu2 lys2 bar1-1*	Singer-Krüger and Ferro-Novick
BS323	*Matα his4 ura3 leu2 lys2 rvs167 bar1-1*	Singer-Krüger and Ferro-Novick
BS325	*Matα his4 ura3 leu2 lys2 sac6 bar1-1*	Singer-Krüger and Ferro-Novick
BS392	*Mat***a** *his3 ura3 leu2 sjl1Δ::URA3 sjl2Δ::LEU2*	This study
BS400	*Matα his3 ura3 leu2 sjl1Δ::URA3 sjl3Δ::HIS3*	This study
BS402	*Matα his3 ura3 leu2 sjl2Δ::LEU2 sjl3Δ::HIS3*	This study
BS551	*Mat***a** *his4 ura3 leu2 lys2 rvs167 bar1-1*	Singer-Krüger and Ferro-Novick
BS582	*Mat***a** *his3 ura3 leu2 lys2 sjl1Δ::URA3 sjl2Δ::LEU2 bar1-1*	This study
BS621	*Mat***a** *his3 ura3 leu2 lys2 sjl2Δ::LEU2 sjl3Δ::HIS3 bar1-1*	This study
BS622	*Mat***a** *his3 ura3 leu2 lys2 sjl1Δ::URA3 sjl3Δ::HIS3 bar1-1*	This study
BS623	*Mat***a** *his3 ura3 leu2 lys2 sjl1Δ::URA3 sjl2Δ::LEU2 bar1-1*	This study
BS624	*Mat***a** *his3 ura3 leu2 sjl2Δ::LEU2 bar1-1*	This study
BS627	*Mat***a** *his3 ura3 leu2 sjl1Δ::URA3*	This study
BS628	*Mat***a** *his3 ura3 leu2 lys2 sjl2Δ::LEU2*	This study
BS631	*Mat***a** *his3 ura3 leu2 sjl3Δ::HIS3*	This study

of them, the gene products of *SJL1*, *SJL2* and *SJL3*, have the same three-domain structure as synaptojanin 1 and 2 (Srinivasan et al., 1997). A first characterization of strains harboring mutations in these genes demonstrated that single mutants display only minor defects, suggesting that each *SJL* gene has a redundant function. However, a variety of phenotypes including abnormal sensitivity to high osmolarity, changes in cell morphology, actin organization and vacuolar morphology were found in some of the double mutants (Srinivasan et al., 1997). Luo and Chang (1997) have also reported that mutations in *SJL3* (referred to as *SOP2*) can suppress the temperature-sensitive growth of a mutant in the plasmalemma ATPase encoded by *PMA1*. In this mutant, *pma1*^{ts}, Pma1p is mislocalized to the vacuole (Chang and Fink, 1995).

The goal of this study was to provide functional evidence for the putative role of synaptojanin family members in endocytosis by analyzing yeast strains lacking *SJL* genes for endocytic defects. We report the occurrence of a major endocytic internalization defect in a Δ*sjl1* Δ*sjl2* mutant and a milder defect in a Δ*sjl2* Δ*sjl3* mutant. The endocytic defects in these mutant strains correlated with defects in actin organization and cell polarity as typically seen in mutants defective in the early stages of endocytosis.*

MATERIALS AND METHODS

Strains and growth conditions

The *S. cerevisiae* strains used are listed in Table 1. Unless otherwise indicated, yeast strains were grown in complete medium (1% yeast extract, 2% peptone and 2% dextrose) (YPD) to early logarithmic phase (0.5-2× 10^7 cells/ml) at 30°C in a rotary shaker. YPD containing 1 M NaCl (hsYPD), as well as medium containing 3% glycerol as a carbon source (YPG), was used to reveal growth defects of the Δ*sjl1* Δ*sjl2* and Δ*sjl2* Δ*sjl3* mutants.

*During the revision of this manuscript Stolz et al. (1998) published a phenotypic analysis of mutants in the *SJL1*, *SJL2* and *SJL3* genes, referred to as *INP51*, *INP52* and *INP53*. These authors reported similar findings concerning the growth characteristics and staining patterns with endocytic dyes of the different double mutants.

Genetic manipulations

Large internal portions of the genes *SJL1*, *SJL2* and *SJL3* were deleted from the genome and replaced with the *URA3*, *LEU2* and *HIS3* genes, respectively. *sjl1::URA3*, which replaced the complete ORF of *SJL1* with the yeast *URA3* gene, was constructed as follows. The 0.2-kb fragments immediately adjacent to the *SJL1* coding region were amplified by PCR (polymerase chain reaction) and subcloned into the yeast integration plasmid pRS306 (Sikorski and Hieter, 1989). The resulting plasmid was digested with *Hin*dIII and the linearized disruption cassette, consisting of the *URA3* gene flanked by the 5′-upstream and 3′-downstream regions of the *SJL1* gene, was transformed into the haploid strain NY1210 or NY1211 by the lithium acetate method (Ito et al., 1983). Stable Ura$^+$ transformants were isolated, and the proper gene replacement was confirmed by PCR analysis (data not shown). The *sjl2::LEU2* and *sjl3::HIS3* disruptions that replaced the complete *SJL2* and *SJL3* ORFs with the yeast *LEU2* and *HIS3* genes were constructed in essentially the same way by using pRS305 and pRS303, respectively (Sikorski and Hieter, 1989). To obtain Δ*sjl* mutants in a *bar1-1* strain background each of the original *sjl* deletion strains was crossed at least three times to either BS64, BS188, or RH2878, which are all isogenic. To generate the *sjl* double mutants, each of the single mutants was mated overnight on YPD plates. The diploids were purified, sporulated and tetrad analysis was performed. The double mutants were identified by the auxotrophic markers (*URA3*, *LEU2* and *HIS3*).

A characterization of the growth properties of these mutants confirmed and extended previous observations made with a different set of mutants (Srinivasan et al., 1997). More specifically, no growth defects were observed in single mutants, as previously reported (Srinivasan et al., 1997). The Δ*sjl1* Δ*sjl2* strain was cold-sensitive (cs) and temperature-sensitive (ts) for growth on rich medium (YPD) at 15°C and 37°C, respectively. In addition, it grew considerably slower than wild type even at the most permissive temperature of 30°C. The Δ*sjl2* Δ*sjl3* double mutant only revealed significant growth deficiencies at 37°C when grown on rich medium containing 1 M NaCl (hsYPD), or on rich medium containing the non-fermentable carbon source glycerol (YPG). The Δ*sjl1* Δ*sjl3* double mutant grew as well as the wild-type strain under the conditions tested.

A diploid strain heterozygous for the three deletions was obtained by crossing a Δ*sjl2* Δ*sjl3* double mutant to a Δ*sjl1* single mutant. After sporulation and tetrad dissection, no Ura$^+$/Leu$^+$/His$^+$ colonies were recovered, while double *sjl* deletions were recovered with the expected frequency. This finding confirms that the simultaneous

inactivation of all three *SJL* genes leads to lethality (Srinivasan et al., 1997).

Genetic interactions between the Δ*sjl* mutants (BS627, BS628, BS631) and mutants in *rvs167* and *sac6* (BS323, and BS325, respectively; Singer-Krüger and Ferro-Novick, 1997) were tested after sporulation and tetrad analysis. Spores were grown at 25°C and the growth of the progeny was analyzed at various temperatures.

Lucifer Yellow CH uptake and FM4-64 labeling

Lucifer Yellow CH (LY) uptake was carried out as described by Singer-Krüger et al. (1995), except that more exhaustive washes were performed to confirm that the labeling at the cell periphery observed in the Δ*sjl1* Δ*sjl2* double mutant was represented by dye trapped in plasma membrane invaginations. FM4-64 labeling was performed as described (Vida and Emr, 1995; Wendland et al., 1996) at either 30°C or 0°C. At the end of the incubations cells were mounted on coverslips coated with concanavalin A to promote adhesion to the glass and examined in a Zeiss axiophot fluorescent microscope.

Internalization and degradation of α-factor

These assays were performed as previously described (Dulic et al., 1991; Singer-Krüger and Ferro-Novick, 1997) using ^{35}S-labeled α-factor, which was prepared from biosynthetically labeled yeast cells that overproduce the pheromone (Singer-Krüger and Ferro-Novick, 1997). Internalization studies were performed by two protocols using strains RH2878, BS582, BS621, BS622, BS623 and BS624. In one protocol, α-factor was added to cells preincubated at 30°C and cell samples were then removed after 1, 5, 10, 15, 30 and 60 minutes at the same temperature. The values in Fig. 2a represent the mean of at least three independent experiments. In the second protocol ('pulse-chase'), α-factor was prebound to cells at 0°C for 1 hour. Cells were then harvested, resuspended in prewarmed (30°C) YPD medium and samples were withdrawn and analyzed as described above. The first protocol, which avoids a 0°C preincubation, was used for a systematic analysis of all mutants due to the cold sensitivity of the Δ*sjl1* Δ*sjl2* mutant. The α-factor degradation assay in the wild type and Δ*sjl2* Δ*sjl3* mutant was performed using the 'pulse-chase' protocol (Dulic et al., 1991). The cell-associated (pH 6.0 sample) and internalized (pH 1.2 sample) pheromone was analyzed following a 1, 7.5, 15, 30, 60 and 90 minute incubation at 30°C.

Invertase secretion

Cells were grown in YPD (5% glucose) overnight to early logarithmic phase at 30°C, washed in YPD (0.1% glucose) and resuspended in YPD (0.1% glucose) at 0.5 OD units/ml to allow for the derepression of invertase. After 1, 40 and 60 minutes of incubation at 30°C, 1 ml samples of the culture were removed, supplemented with NaN_3 (10 mM final concentration), shifted to 0°C, washed with ice-cold 10 mM NaN_3, and processed for the analysis of total and external invertase activity by the method of Goldstein and Lampen (1975).

Visualization of the actin cytoskeleton, bud scars and mitochondria

Approximately 20-50 ml of each cell culture were fixed during a 15 minute incubation in 4% formaldehyde. The cells were harvested, incubated further in buffered 4% formaldehyde for 1 hour and resuspended (1-2× 10^7 cells/ml) in PBS. 40 μl of the cell suspension was stained by the addition of 5 μl of rhodamine-phalloidin (Molecular Probes, Eugene, OR) (6.6 μM stock in methanol) and 5 μl of calcofluor (1 mg/ml stock in H_2O) (1 hour at room temperature) followed by several washes in PBS. Cells were immediately viewed on concanavalin A-coated coverslips. To visualize nuclei, fixed cells were incubated for 1 hour at room temperature in 10 mg/ml DAPI. Mitochondria were visualized in living cells. Approximately 0.2 OD_{600} units of an early logarithmic culture were stained with $DiOC_6$ (250 ng/ml) and Mitotracker Red (0.2 μM) (Molecular Probes, Eugene, OR) in YPD under conditions that preferentially label yeast mitochondria (Pringle et al., 1989) and, after embedding in low-melting agarose, viewed by fluorescence microscopy using a Zeiss axiophot microscope.

Electron microscopy

Conventional electron microscopy (EM) was performed as described (Rieder et al., 1996) on cells grown at 30°C to early logarithmic phase.

RESULTS

Fluid-phase endocytosis is defective in the Δ*sjl1* Δ*sjl2* and Δ*sjl2* Δ*sjl3* double mutants

Fluid phase endocytosis was monitored with the fluorescent marker Lucifer Yellow CH (LY). As previously reported (Riezman, 1985), incubation of wild-type yeast cells with LY for 1 hour at 30°C resulted in its accumulation in the vacuole and in a bright selective labeling of this organelle (Fig. 1a,a′). Similar results were obtained with the single mutants and with the Δ*sjl1* Δ*sjl3* double mutant (Fig. 1c,c′). In Δ*sjl1* Δ*sjl2*, no vacuolar accumulation of LY was observed and LY labeling was confined to peripheral punctate-like structures which dimmed after extensive washings at 0°C (Fig. 1b,b′), and thus probably reflected dye trapped in invaginations of the plasma membrane (see below). In the Δ*sjl2* Δ*sjl3* double mutant (Fig. 1d,d′), only a very weak LY labeling of the vacuoles was observed. The results are consistent with the occurrence of an endocytic defect in the Δ*sjl1* Δ*sjl2* and the Δ*sjl2* Δ*sjl3* double mutants, although the nature of the defect appears to differ in the two strains.

Receptor-mediated endocytosis is abnormal in the Δ*sjl1* Δ*sjl2* and Δ*sjl2* Δ*sjl3* double mutants

Receptor-mediated endocytosis was analyzed by measuring the internalization of the mating pheromone α-factor (Fig. 2a) (Dulic et al., 1991). After a short preincubation at 30°C, cells were exposed to ^{35}S-α-factor at the same temperature and the percentage of ^{35}S-labeled pheromone which had become inaccessible to an acid wash after various times was determined. As shown in Fig. 2a, uptake of ^{35}S-α-factor by the Δ*sjl1* Δ*sjl3* mutant as well as the Δ*sjl2* mutant was comparable to wild type and approached approximally 100% after 30 minutes of internalization. In the Δ*sjl2* Δ*sjl3* mutant, the initial rate of ^{35}S-α-factor internalization was lower when compared to wild type ($t_{1/2}$ = 7.5 minutes as compared to 5 minutes), and after 60 minutes of incubation only approximately 70% of the mating pheromone had been internalized. In the Δ*sjl1* Δ*sjl2* mutant the overall rate of internalization was even more severely impaired ($t_{1/2}$ = 18.5 minutes). Although the proportion of acid-resistant ^{35}S-α-factor at the earliest time point (1 minute) was relatively high (see below for discussion), little further increase in apparent ^{35}S-α-factor internalization was observed at the 60 minutes time point. The temperature at which these defects were observed (30°C) was permissive for the growth of both mutants. When α-factor internalization was performed at 37°C, the endocytosis defect in the Δ*sjl2* Δ*sjl3* mutant was only slightly aggravated (data not shown). The same experiment could not be performed for the Δ*sjl1* Δ*sjl2* strain, due to the poor growth of this strain at 37°C. A comparable inhibition of α-factor internalizaton in the Δ*sjl2* Δ*sjl3* and the Δ*sjl1* Δ*sjl2* mutants was observed when the uptake assay was performed using a 'pulse-chase' protocol,

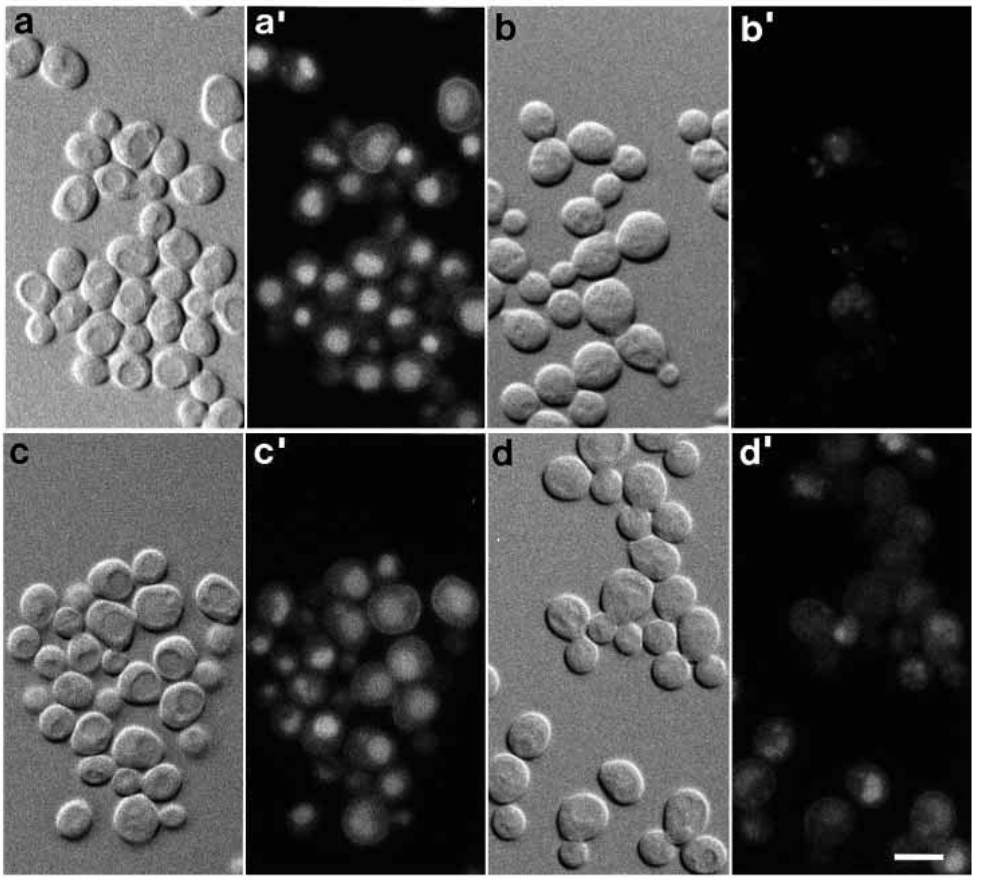

Fig. 1. Accumulation of LY is altered in two Δ*sjl* double mutants. LY internalization was performed at 30°C for 1 hour. Subsequently, the cells were washed with ice-cold buffer in the presence of NaN_3, mounted in low melting agarose and visualized using fluorescence (right panels) and Nomarski optics (left panels). (a) Wild type; (b) Δ*sjl1* Δ*sjl2*; (c) Δ*sjl1* Δ*sjl3*; (d) Δ*sjl2* Δ*sjl3*. Bar, 5 μm.

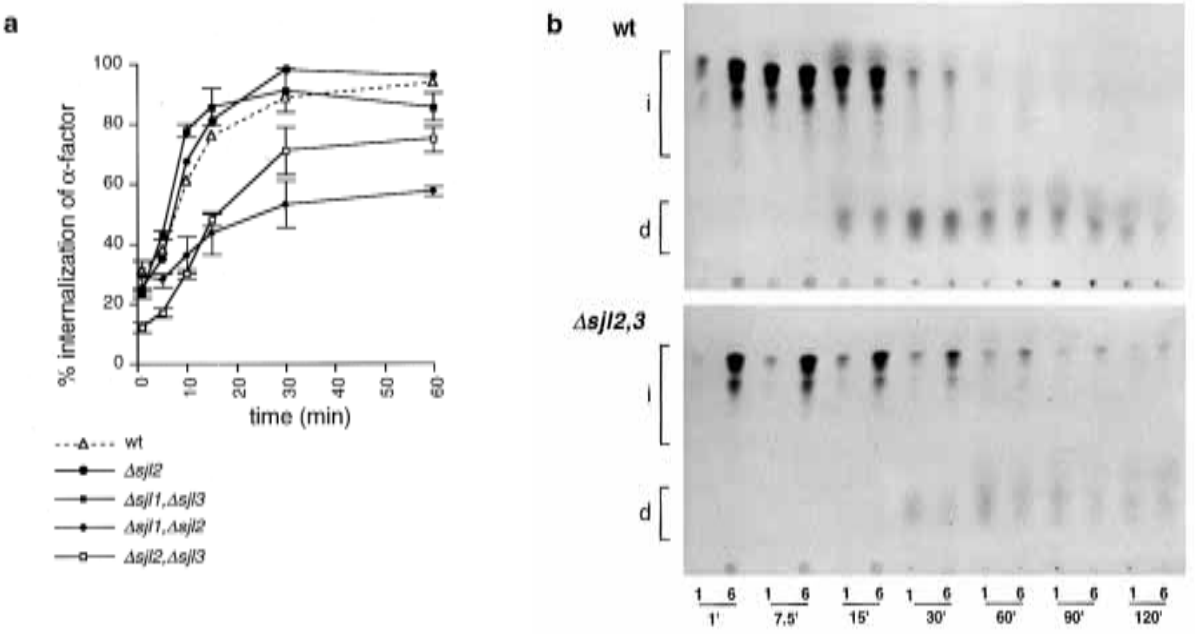

Fig. 2. Kinetics of α-factor internalization and degradation in Δ*sjl* double mutants. (a) Cells of the a mating type were preincubated in YPD medium for 15 minutes at 30°C before ^{35}S-α-factor was added and the incubation continued at 30°C. At the indicated times, samples were withdrawn and processed as described in the Materials and Methods. (b) Wild-type and Δ*sjl2* Δ*sjl3* cells were incubated with ^{35}S-α-factor for 1 hour on ice. Subsequently, cells were collected, resuspended in prewarmed YPD medium (30°C) and transferred to a 30°C waterbath. At the indicated times, samples were withdrawn and processed as described in Materials and methods. Total cell-associated (pH 6.0 washed cells) (6) and internalized α-factor (pH 1.2 washed cells) (1) were extracted at the indicated times and resolved by thin-layer chromatography. The positions of intact (i) and degraded (d) pheromone are indicated. The fluorograms were exposed for 10 days at −70°C. (a) wild type; (b) Δ*sjl2* Δ*sjl3*.

which involves preincubation of the cells with the pheromone at 0°C followed by a shift to 30°C.

In wild-type cells, internalized α-factor is transported via two distinct endosomal intermediates to the vacuole, where it is finally degraded (Singer and Riezman, 1990; Singer-Krüger et al., 1993). Since the Δ*sjl2* Δ*sjl3* double mutant internalized pheromone after 60 minutes of incubation, we determined whether internalized ^{35}S-α-factor underwent normal degradation, i.e. was transported to the vacuole. The degradation of α-factor at different time points of internalization was assessed by separating intact and degraded forms by thin-layer chromatography. In wild-type cells the majority of pheromone was degraded approximately 30 minutes after internalization, as revealed by the disappearance of intact α-factor and by the concomitant appearance of degradation products (Fig. 2b). This process was only slightly delayed in the Δ*sjl2* Δ*sjl3* mutant. Such a delay, however, could be an indirect consequence of the slower rate of pheromone internalization and may not represent a disruption of the endocytic pathway from the cell surface to the vacuole.

Abnormal labeling with FM4-64 in the Δ*sjl1* Δ*sjl2* mutant

Another method that has been used to monitor endocytosis in yeast is uptake of the fluorescent, amphipathic dye FM4-64 (Vida and Emr, 1995). FM4-64 is soluble in water, accumulates very efficiently into membranes, but does not cross the bilayer. When added to wild-type cells at 0°C, it selectively labels the cell surface and the surface-bound dye can be rapidly removed by washing. At physiological temperatures it is rapidly internalized and transported to the vacuole.

Previously, it was reported that at 30°C the uptake of FM4-64 by Δ*sjl* single mutants and Δ*sjl1* Δ*sjl3* and Δ*sjl2* Δ*sjl3* double mutants was qualitatively similar to wild-type (Srinivasan et al., 1997). Surprisingly, a very high level of FM4-64 labeling on vacuolar-like structures was also observed in the Δ*sjl1* Δ*sjl2* mutant at this temperature (Srinivasan et al., 1997). This result appears to contradict the endocytosis internalization defect of this strain reported in Figs 1 and 2a. Incubations at 0°C were therefore performed to determine whether the structures labeled by FM4-64 in the Δ*sjl1* Δ*sjl2*

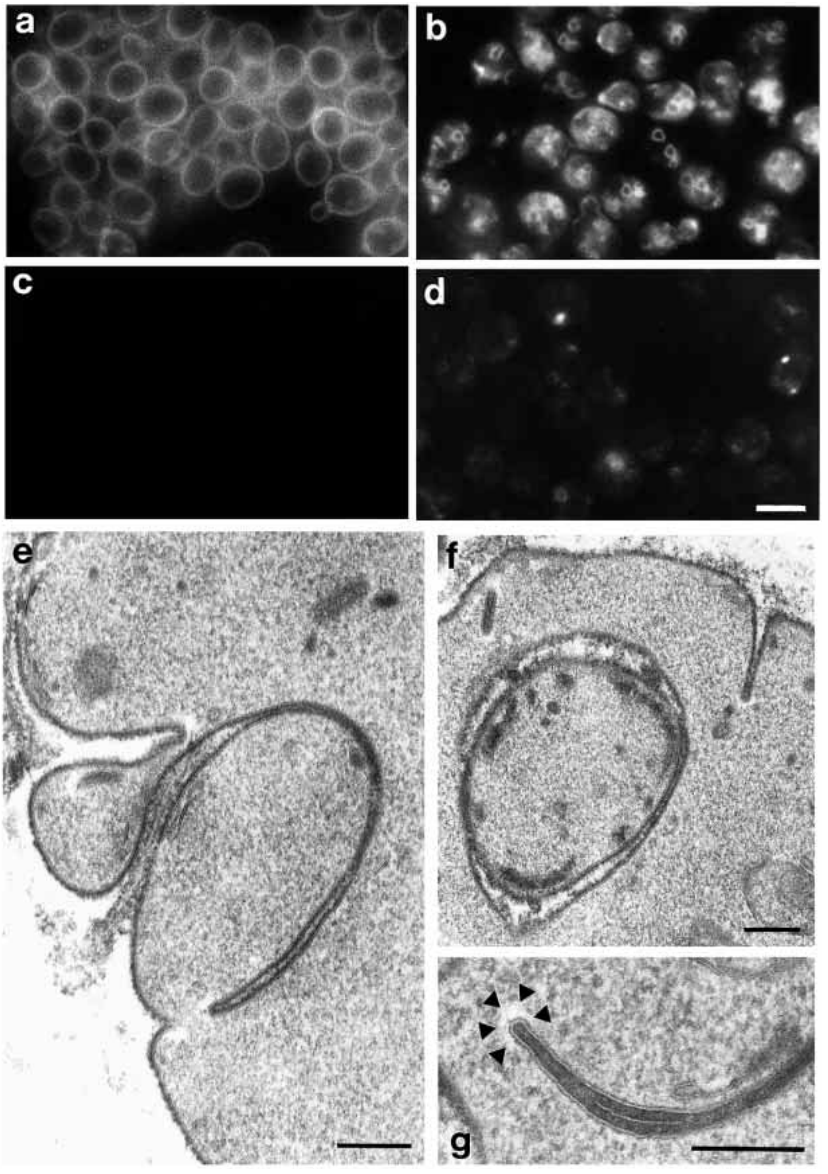

Fig. 3. Presence of vacuolar-like invagination exposed to the extracellular space in the *Δsjl1 Δsjl2* strain. (a-d) Wild-type (a,c) and *Δsjl1 Δsjl2* (b,d) cells were labeled with FM4-64 at 0°C for 30 minutes and photographed either immediately (a,b) or after a 60 minute wash at the same temperature (c,d). Prior to washing (a,b) only the outer cell profile is labeled in wild-type cells, while intense labeling of apparently intracellular ring-like structures is visible in the *Δsjl1 Δsjl2* double mutants. The outer cell profile is hardly visible in field b due to a shorter photographic exposure than for wild-type cells. Both the label of wild-type cells and most of the label of the *Δsjl1 Δsjl2* strain disappears after washing, suggesting that the vacuolar-like labeling of this strain represents invaginations of the cell surface. (e-g) Electron micrographs of Δ*sjl1* Δ*sjl2* spheroplasts. (e,f) Invaginations of the cell surface which fold upon themselves (e) to generate vacuolar-like structures surrounded by a double membrane (e,f). (g) High power view of the tip of one of the infoldings. Arrowheads indicate a clear region of the cytoplasm, suggesting the presence of a coat structure. Bars, 5 μm (a-d); 200 nm (e,f,g).

strain represent bona fide endocytic vesicles or invaginations of the cell surface. Addition of FM4-64 at 0°C resulted in the labeling of the typical yeast surface profile in wild-type cells (Fig. 3a). A similar staining was also observed in Δ*sjl2* Δ*sjl3* and Δ*sjl1* Δ*sjl3* cells (data not shown). In contrast, a massive vacuole-like labeling, in addition to labeling of the outer cell profile, was observed within seconds after addition of the dye in the Δ*sjl1* Δ*sjl2* strain (Fig. 3b). However, not only the labeling of the outer cell profile, but also most of the internal-like labeling of Δ*sjl1* Δ*sjl*2 cells could be removed by extensive washings at 0°C (Fig. 3d). Thus, the seemingly 'internal' labeling does not reflect segregation of the dye into bona fide intracellular vesicles.

The structures labeled by FM4-64 at 0°C in the Δ*sjl1* Δ*sjl2* double mutant are likely to represent the vacuolar-like profiles previously described by electron microscopy in this mutant. The plasmalemma of this strain forms deep invaginations, which often fold onto themselves to almost completely enwrap portions of the cytoplasm. As a consequence, structures are generated that in many planes of sections appear as islands of cytoplasm surrounded by two membranes (Srinivasan et al., 1997; Fig. 3e-g). However, as demonstrated by *in vivo* labeling of spheroplasts with cationized ferritin (a membrane-impermeant electron microscopy marker for endocytosis; Herzog and Farquhar, 1983; Wendland et al., 1996), the space between these membranes was clearly continuous with the cell surface, even when the continuity was not visible in the plane of section (not shown).

For comparison, we also examined the ultrastructural morphology of a well-established yeast endocytic internalization mutant, *rvs167* (Munn et al., 1995; Singer-Krüger and Ferro-Novick, 1997). Although the Δ*sjl1* Δ*sjl2* and the *rvs167* mutants are similarly impaired in the internalization of α-factor, the *rvs167* mutant did not reveal the deep invaginations of the plasma membrane that are present in the Δ*sjl1* Δ*sjl2* mutant (data not shown).

Invertase secretion is not affected in Δ*sjl* mutants

To determine whether the endocytic defect of the Δ*sjl1* Δ*sjl2* and Δ*sjl2* Δ*sjl3* strains reflects a general inhibition of membrane traffic at the cell surface, we assayed the secretion of invertase. Cells were grown in high glucose medium to repress the *SUC2* gene encoding invertase, and then *SUC2* was derepressed by shifting to low glucose medium. 40 and 60 minutes after the shift, total and external invertase activities were determined. In the Δ*sjl1* Δ*sjl3* mutant, the level of invertase induction was comparable to wild-type cells, while it was somewhat reduced in the Δ*sjl2* Δ*sjl3* and Δ*sjl1* Δ*sjl2* strains (data not shown). All mutant strains, however, retained the ability to secrete invertase into the periplasmic space, since the ratios of external invertase activity to total invertase activity were in a similar range (0.83 in wild type, 0.87 in Δ*sjl1* Δ*sjl2*, 0.82 in Δ*sjl2* Δ*sjl3* and 0.79 in Δ*sjl1* Δ*sjl3*). This finding argues against an essential direct role of Sjl1p, Sjl2p and Sjl3p in the secretory pathway, including exocytosis.

Budding polarity defects in Δ*sjl1* Δ*sjl2* and Δ*sjl2* Δ*sjl3* mutants

A correlation has been observed in a variety of yeast mutant strains between endocytic internalization defects, defects in actin organization and abnormal cell polarity. In view of the endocytic (see above) and actin organization (Srinivasan et al., 1997) defects of the Δ*sjl1* Δ*sjl2* and Δ*sjl2* Δ*sjl3* double mutants, we examined the polarity of budding in these mutants.

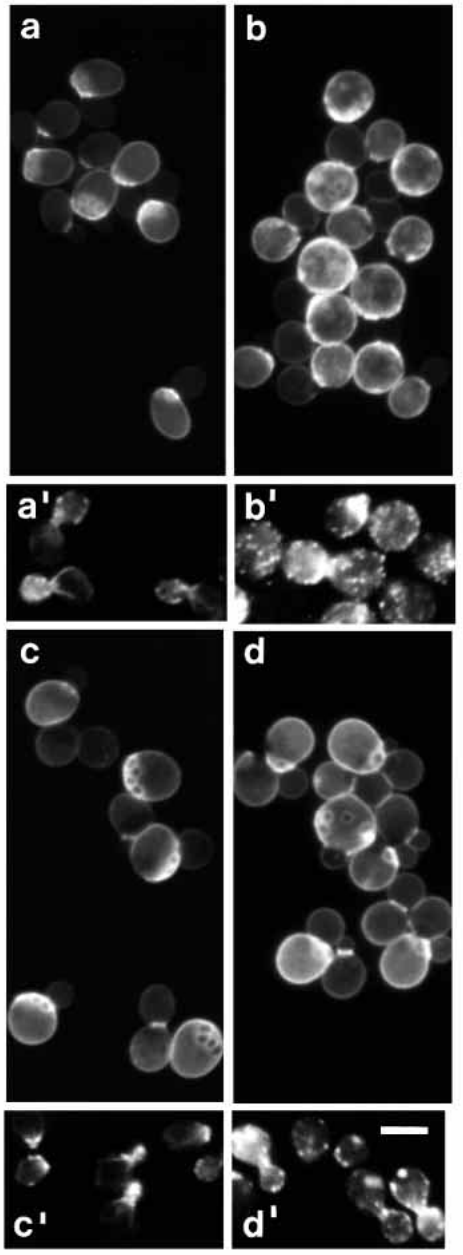

Fig. 4. The Δ*sjl1* Δ*sj2* and Δ*sjl2* Δ*sjl3* mutants reveal an altered budding pattern in haploid cells which correlates with abnormal actin organization. Wild-type and Δ*sjl* double mutants were fixed with formaldehyde and stained either with the fluorescent dye calcofluor (a-d) or rhodamine-phalloidin (a′-d′). (a) Wild-type; (b) Δ*sjl1* Δ*sjl2*; (c) Δ*sjl1* Δ*sjl3*; (d) Δ*sjl2* Δ*sjl3*. Bar, 4.5 μm (a-d) and 5 μm (a′-d′).

S. cerevisiae exhibits stereotypic patterns of bud site selection. Haploid cells display an axial budding pattern in which the new bud is adjacent to the previous one, while diploids bud in a bipolar pattern from either pole (Chant and Pringle, 1995). This process can be monitored by staining chitin with the fluorescent dye calcofluor. The budding pattern was clearly axial in wild-type (Fig. 4a) and Δ*sjl1* Δ*sjl3* haploid

cells (Fig. 4c), in agreement with a normal organization of the actin cytoskeleton in these strains (actin patches concentrated in the bud or daughter cells and actin cables aligned along the mother-daughter cell axis) (Fig. 4a′,c′). In contrast, budding polarity was completely lost in the Δ*sjl1* Δ*sjl2* strain (Fig. 4b), in which actin patches were randomly distributed throughout the mother-daughter cell (Fig. 4b′). Chitin rings appeared smaller than normal and the diffuse cell surface labeling for chitin was brighter than in wild-type cells (Fig. 4b). In the Δ*sjl2* Δ*sjl3* mutant, a less severe disruption of budding polarity was observed together with some enhanced diffuse chitin labeling. In this mutant, most, but not all, chitin rings were adjacent to each other (Fig. 4d). Although the Δ*sjl2* Δ*sjl3* mutant displayed an unpolarized distribution of actin cortical patches similar to the Δ*sjl1* Δ*sjl2* strain, the aberrant actin patches in the former strain were clearly larger and less numerous (compare Fig. 4d′ with Fig. 4b′). In summary, Δ*sjl1* Δ*sjl2* and Δ*sjl2* Δ*sjl3* mutants display defects in bud site selection during polarized cell growth consistent with defects in the organization of the actin cytoskeleton. The phenotypically distinct defects in polarity and actin organization revealed between the Δ*sjl1* Δ*sjl2* and Δ*sjl2* Δ*sjl3* mutants suggest distinct roles of synaptojanin family members in actin function (see also below).

SJL1 genetically interacts with *SAC6*

In view of the effect of *SJL* mutations on actin organization and on the internalization step of endocytosis, we searched for an interaction between the *SJL* genes and two other genes implicated in actin function and endocytosis: *SAC6* (Kübler and Riezman, 1993) and *RVS167* (Munn et al., 1995). These two genes encode the yeast homologs of fimbrin (an actin bundling protein) (Adams and Botstein, 1989) and amphiphysin (David et al., 1994), respectively.

Each Δ*sjl* single mutant was crossed to *sac6* and *rvs167* mutants, respectively. After sporulation and dissection of the heterozygous diploids, the colonies that were derived from each of the four spores were grown up at 25°C. Subsequently, growth was analyzed at various temperatures (30°C, 35°C and 37°C). Strikingly, at 37°C, the restrictive temperature for the *sac6* mutant, the growth defect was partially suppressed by the deletion of *SJL1*, but not by the deletion of *SJL2* nor *SJL3* (Fig. 5). Strains carrying a mutation in *RVS167* in combination with the deletion of each of the *SJL1*, *SJL2* and *SJL3* genes, respectively, did not exhibit a growth phenotype that was markedly different from that displayed by each of the single mutants. Finally, overexpression of *SAC6*, *ACT1* (which encodes yeast actin), *RVS167* and *RVS161* (a homologue of *RVS167*) (the latter two genes individually or in combination), did not rescue the growth defects of the Δ*sjl1* Δ*sjl2* and the Δ*sjl2* Δ*sjl3* double mutants. The genetic interaction between *SJL1* and *SAC6* strongly suggests that the products of these genes may have opposing effects on the actin cytoskeleton.

The Δ*sjl1* Δ*sjl2* mutant exhibits aberrant mitochondrial organization

As part of a systematic characterization of the Δ*sjl* mutant strains, we stained cells with DAPI, a DNA-specific dye. This revealed normal nuclear localization and segregation during cell division. Surprisingly, the mitochondria, which were also stained by DAPI, revealed an abnormal morphology in the Δ*sjl1* Δ*sjl2* double mutant. This phenotype was confirmed by mitochondrial labeling with the vital dyes $DiOC_6$ (Fig. 6) and mitotracker (not shown). While mitochondria exhibited the typical tubule-like structure in wild type (Fig. 6a,a′) and the Δ*sjl1* Δ*sjl3* and Δ*sjl2* Δ*sjl3* mutants (not shown), they appeared as random dots in the Δ*sjl1* Δ*sjl2* strain (Fig. 6b,b′). It is important to note that mitochondrial morphology, which is tightly linked to actin function (Drubin et al., 1993), was not affected in the Δ*sjl2* Δ*sjl3* mutant, in spite of the aberrant actin

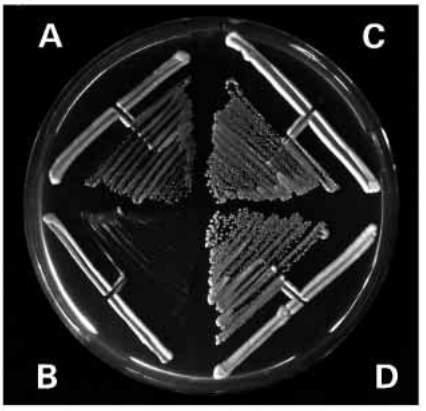

Fig. 5. Deletion of *SJL1* suppresses the temperature-sensitive growth phenotype of *sac6*. A mutant in *sac6* (BS325; Singer-Krüger and Ferro-Novick, 1997) was crossed to Δ*sjl1* (BS627). After sporulation of the heterozygous diploid, tetrad analysis was performed on colonies that grew at 25°C. *sac6* and Δ*sjl1* were followed by the ts growth and Ura^+ phenotypes, respectively. One representative tetrad is shown. (a) *sac6* Δ*sjl1*; (b) *sac6*; (c) Δ*sjl1*; (d) wild type.

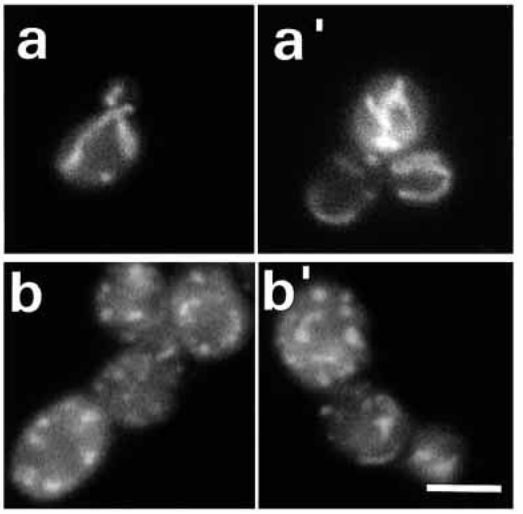

Fig. 6. Abnormal mitochondrial morphology in the Δ*sjl1* Δ*sjl2* double mutant. Cells were incubated at room temperature for approximately 3 minutes with $DiOC_6$ and immediately examined. (a,a′) Two different fields of wild type; (b,b′) two different fields of Δ*sjl1* Δ*sjl2*. Bar, 5 μm.

cytoskeleton staining pattern in this strain (Fig. 4d). It should also be noted that mitochondria were present in the growing buds of all the three *sjl* double mutants including Δ*sjl1* Δ*sjl2*. This indicates that mitochondrial inheritance, another process which involves actin (Drubin et al., 1993), is preserved.

DISCUSSION

The goal of this study was to use yeast genetics to test the hypothesis that synaptojanin family members play a role in endocytosis, consistent with the proposed role of synaptojanin 1 in the endocytosis of synaptic vesicles (McPherson et al., 1994b; Haffner et al., 1997). To this aim we have tested the effect of *SJL* deletions on fluid-phase and receptor-mediated endocytosis. We report the occurrence of an endocytosis defect in the Δ*sjl2* Δ*sjl3* mutant and of a severe impairment of endocytosis in the Δ*sjl1* Δ*sjl2* mutant. In either strain both fluid-phase uptake (LY) and receptor-mediated endocytosis (α-factor internalization) were affected, suggesting an impairment of some key aspect of the endocytic machinery. However, the different phenotypes of the two mutants indicate at least partially distinct defects rather than a different penetrance of the same defect.

A profound alteration of the cellular morphology, with a massive increase of the cell surface area, occurs exclusively in the Δ*sjl1* Δ*sjl2* mutant. Deep invaginations of the plasma membrane must reflect an imbalance between exocytosis and endocytosis which is not compensated by a parallel increase in overall growth. Our data strongly support the hypothesis that the invaginations of the Δ*sjl1* Δ*sjl2* strain result from a selective impairment of endocytosis, because secretion of invertase was found to occur at wild-type levels. Although the plasma membrane invaginations were clearly unique to the Δ*sjl1* Δ*sjl2* mutant, they could represent an exaggeration of furrow-like invaginations often visible even in wild-type cells (Prescianotto-Baschong and Riezman, 1998). These invaginations appear to be the sites at which receptor-mediated endocytosis takes place (J. Mulholland and D. Botstein, personal communication). Since Δ*sjl2* Δ*sjl3* and *rvs167* do not exhibit the abnormal surface invaginations, a balance between exocytosis and endocytosis is likely to be maintained in these mutants, as in several previously reported endocytosis mutants (Raths et al., 1993; Kübler and Riezman, 1993; Munn et al., 1995), in spite of the kinetic delay in endocytosis. In some other endocytosis mutants, however, a moderate deepening of normal cell surface invaginations was observed (Prescianotto-Baschong and Riezman, 1998; Wendland et al., 1996).

Very deep and narrow plasmalemmal infoldings, reminiscent of those present in the *Δsjl1 Δsjl2* cells, were previously observed in *Drosophila melanogaster* and mammalian cells in which dynamin function is impaired by mutations, transfection or antibody injections (Koenig and Ikeda, 1990; Damke et al., 1995; Henley et al., 1998). Thus, the consequence of the simultaneous deletion of *SJL1* and *SJL2* on cell surface morphology of yeast cells is consistent with the putative link between the function of dynamin and synaptojanin 1 in mammals (McPherson et al., 1994b, 1996; Haffner et al., 1997; Mundigl et al., 1998). In animal cells with impaired dynamin function these infoldings often terminate in a clathrin-coated bud (Koenig and Ikeda, 1990; Henley et al., 1998), as if the infolding were generated by the internalization of a bud which cannot undergo fission. It is of interest that the tips of surface infoldings in the Δ*sjl1* Δ*sjl2* mutant also have a peculiar cytoplasmic undercoating which appears as an unstained area (arrowheads in Fig. 3g).

The plasmalemmal invaginations of the Δ*sjl1* Δ*sjl2* mutant generate 'pseudo-intracellular compartments'. This ultrastructural feature may explain some of the puzzling results obtained by the classical endocytosis assays. The spots of LY that were visible at the cell periphery of mutant cells after exposure to the dye may represent partially trapped LY which had not been truly internalized, since most of the dye could be removed by extensive washes at 0°C in the presence of NaN_3. Likewise, α-factor trapped in these compartments may be artifactually scored as 'internalized' by the endocytosis assay and may contribute to the higher level of uptake at 1 minute, in spite of minimal further uptake. Furthermore, accumulation of FM4-64 was enhanced, rather than decreased, in the mutant, due to the concentration of this amphipatic dye in the invaginations. Therefore, although decreased cellular labeling by FM4-64 was successfully used to isolate new yeast endocytosis mutants (Wendland et al., 1996), at least one such mutant exhibits an opposite phenotype in this assay (see also Srinivasan et al., 1997).

In agreement with a putative regulatory role of phosphoinositides on the function of the actin cytomatrix (Janmey, 1994), we show that Δ*sjl1* Δ*sjl2* and Δ*sjl2* Δ*sjl3* mutants exhibit budding polarity defects which correlate with morphological alterations of the actin cytoskeleton. Again, reproducible differences in both actin organization and chitin distribution were observed in the two mutants, indicating that distinct synaptojanins have specific functions in these processes. Deletion of *SJL1*, but not of *SJL2* and *SJL3*, led to the suppression of the temperature-sensitive growth defect of a *sac6* mutant strongly indicating a functional link between Sjl1p and actin function. Sac6p, which is 43% identical to mammalian fimbrin, promotes actin filament assembly and binds to actin in vivo (Adams et al., 1991). Furthermore, it is essential for the internalization step of endocytosis (Kübler and Riezman, 1993). Similar to our finding that Δ*sjl1* can suppress *sac6*, it has been previously shown that mutants in *act1* can suppress *sac6* and vice versa (Adams and Botstein, 1989; Adams et al., 1989; Novick and Botstein, 1985). The correlation between endocytic defects, actin cytoskeleton disruption and loss of cell polarity observed for a variety of yeast mutants (Riezman et al., 1996) indicates that these processes are functionally interrelated. Growing evidence suggests that in mammalian cells both clathrin-dependent and clathrin-independent endocytosis also require the proper function of the actin cytoskeleton (Lamaze et al., 1997; Mundigl et al., 1998; Schmalzing et al., 1995).

The distinct phenotypes displayed by Δ*sjl1* Δ*sjl2* and Δ*sjl2* Δ*sjl3* not only include endocytosis, plasma membrane morphology and cellular polarity, but also growth (see Materials and Methods). Based on these phenotypes it appears that Sjl2p is the most critical member of three yeast synaptojanin-like proteins for cell physiology, followed by Sjl1p and Sjl3p. The cold- and temperature-sensitive growth phenotypes displayed by Δ*sjl1* Δ*sjl2*, and Δ*sjl2* Δ*sjl3*, respectively, can now be exploited in genetic screens to identify genes with a related function to synaptojanins in yeast.

An unexpected phenotype of the Δ*sjl1* Δ*sjl2* double mutant was an abnormal mitochondrial morphology. This effect may be indirect and caused by the deep invaginations of the cell surface which may perturb the normal tubulo-reticular structure of yeast mitochondria. However, in view of the suggested functional relationship between synaptojanin 1 and dynamin in mammalian cells, it is of interest that yeast strains harboring mutations in either one of two genes homologous to dynamin, *MGM1* and *DNM1* (Jones and Fangman, 1992; Gammie et al., 1995), also exibit an abnormal mitochondrial organization (Jones and Fangman, 1992; Guan et al., 1993; Shaw et al., 1997). Since dynamin function has been linked to actin (Witke et al., 1998; Damke et al., 1995; De Camilli et al., 1995), it is possible that the abnormal mitochondrial morphology in Δ*sjl1* Δ*sjl2*, *mgm1*, and *dnm1* may be caused by defects in the actin cytoskeleton in these mutants.

In conclusion, our data demonstrate that the multiple phenotypes of two *sjl* double mutants include endocytic defects. These findings provide the first functional piece of evidence supporting the putative role of mammalian synaptojanin 1, and more generally of phosphoinositide metabolism, in endocytosis. Lack of major defects in *sjl* single mutants clearly demonstrate that the *SJL* genes have redundant functions. Nevertheless, the distinct phenotypes exhibited by the three different double mutants also indicate that the *SJL* genes have only partially overlapping roles and act on distinct pools of inositol metabolites. This is consistent with the evolutionary divergence of the three genes at their COOH-terminal domains, i.e. the domains which are thought to play an important role in subcellular targeting. It should be noted that Sjl2p, which our studies suggest as the most critically required synaptojanin family member for endocytosis, is the Sjl protein more closely related in overall structure and primary amino acid sequence to synaptojanin 1. An interplay of yeast studies and studies on vesicle recycling at the synapse and in other systems of higher eukaryotes will help to further elucidate the function of each member of the synaptojanin family.

We thank Dr Janet Burton for help in preliminary experiments and Dr Peter Novick for strains, advice and discussion. We are grateful to Dr Howard Riezman for providing a strain. This work was supported in part by grants from the NIH (CA46128 to P. D. C. and S. F. N. and NS36251 to P. D. C., the HFSP (P. D. C.), the United States Army Medical Research and Development Command (P. D. C.) and a fellowship from the Patrick and Catherine Weldon Donaghue Medical Research Foundation (B. S.-K.)

REFERENCES

Adams, A. E. M., Botstein, D. and Drubin, D. G. (1989). A yeast actin-binding protein is encoded by *SAC6*, a gene found by suppression of an actin mutation. *Science* **243**, 231-233.

Adams, A. E. and Botstein, D. (1989). Dominant suppressors of yeast actin mutations that are reciprocally suppressed. *Genetics* **121**, 675-683.

Adams, A. E. M., Botstein, D. and Drubin, D. G. (1991). Requirement of yeast fimbrin for actin organization and morphogenesis in vivo. *Nature* **354**, 404-408.

Bauerfeind, R., Takei, T. and De Camilli, P. (1997). Amphiphysin I is associated with coated endocytic intermediates and undergoes stimulation-dependent dephosphorylation in nerve terminals. *J. Biol. Chem.* **272**, 30984-30992.

Berridge, M. J. (1997). Elementary and global aspects of calcium signalling. *J. Physiol.* **499**, 290-306.

Chang, A. and Fink, G. R. (1995). Targeting of the yeast plasma membrane H^+ATPase: a novel gene *AST1* prevents mislocalization of mutant ATPase to the vacuole. *J. Cell. Biol.* **128**, 39-49.

Chant, J. and Pringle, J. R. (1995). Patterns of bud-site selection in the yeast *Saccharomyces cerevisiae. J. Cell Biol.* **129**, 751-765.

Cleves, A. E., Novick, P. J. and Bankaitis, V. A. (1989). Mutations in the *SAC1* gene suppress defects in yeast Golgi and yeast actin function *J. Cell Biol.* **109**, 2939-2950.

Cremona, O. and De Camilli, P. (1997). Synaptic vesicle endocytosis. *Curr. Opin. Neurobiol.* **7**, 323-330.

Damke, H., Baba, T., van der Bliek, A. M. and Schmid, S. L. (1995). Clathrin-independent pinocytosis is induced in cells overexpressing a temperature-sensitive mutant of dynamin. *J. Cell Biol.* **131**, 69-80.

David, C., Solimena, M. and De Camilli, P. (1994). Autoimmunity in Stiff-Man Syndrome with breast cancer is targeted to the C-terminal region of human amphiphysin, a protein similar to the yeast proteins, Rvs167 and Rvs161. *FEBS Lett.* **351**, 73-79.

David, C., McPherson, P. S., Mundigl, O. and De Camilli, P. (1996). A role of amphiphysin in synaptic vesicle endocytosis suggested by its binding to dynamin in nerve terminals. *Proc. Nat. Acad. Sci. USA* **93**, 331-335.

De Camilli, P., Takei, K. and McPherson, P. S. (1995). The function of dynamin in endocytosis. *Curr. Opin. Neurobiol.* **5**, 559-565.

De Camilli, P., Emr, S. D., McPherson, P. S. and Novick, P. (1996). Phosphoinositides as regulators in membrane traffic. *Science* **271**, 1533-1539.

de Heuvel, E., Bell, A. W., Ramjaun, A. R., Wong, K., Sossin, W. S. and McPherson, P. S. (1997). Identification of the major synaptojanin-binding proteins in brain. *J. Biol. Chem.* **272**, 8710-8716.

Drubin, D. G., Jones, H. D. and Wertman, K. F. (1993). Actin structure and function: roles in mitochondrial organization and morphogenesis in budding yeast and identification of the phalloidin-binding site. *Mol. Biol. Cell* **4**, 1277-1294.

Dulic, V., Egerton, M., Elguindi, I., Raths, S., Singer, B. and Riezman, H. (1991). Yeast endocytosis assays. *Meth. Enzymol.* **194**, 679-710.

Gammie, A. E., Kurihara, L. J., Vallee, R. B. and Rose, M. D. (1995). *DNM1*, a dynamin-related gene, participates in endosomal trafficking in yeast. *J. Cell Biol.* **130**, 553-566.

Goffeau, A. et al. (1997). The yeast genome directory. *Nature* **387**, 5-105.

Goldstein, A. and Lampen, J. O. (1975). Beta-D-fructofuranoside fructohydrolase from yeast. *Methods Enzymol.* **42**, 504-511.

Guan, K., Farh, L., Marshall, T. K. and Deschenes, R. J. (1993). Normal mitochondrial structure and genome maintanance in yeast requires the dynamin-like product of the *MGM1* gene. *Curr. Genet.* **24**, 141-148.

Haffner, C., Takei, K., Chen, H., Ringstad, N., Hudson, A., Butler, N. H., Salcini, A. E., Di Fiore, P. P. and De Camilli, P. (1997). Synaptojanin 1: localization on coated endocytic intermediates in nerve terminals and interaction of its 170 kDa isoform with Eps15. *FEBS lett.* **419**, 175-180.

Henley, J. R., Krueger, E. W. A., Oswald, B. J. and McNiven, M. A. (1998). Dynamin-mediated internalization of caveolae. *J. Cell. Biol.* **141**, 85-99.

Herzog and Farquhar (1983). *Meth. Emzymol.* **98**, 203-225.

Ito, H., Fukada, Y., Murata, K. and Kimura, A. (1983). Transformation of intact yeast cells treated with alkali cations. *J. Bacteriol.* **153**, 163-168.

Janmey, P. A. (1994). Phosphoinositides and calcium as regulators of cellular actin assembly and disassembly. *Ann. Rev. of Physiol.* **56**, 169-191.

Jefferson, A. B., Auethavekiat, V., Pot, D. A., Williams, L. T. and Majerus, P. W. (1997). Signaling inositol polyphosphate-5-phosphatase. Characterization of activity and effect of Grb2 association. *J. Biol. Chem.* **272**, 5983-5988.

Jones, B. A. and Fangman, W. L. (1992). Mitochondrial DNA maintanance in yeast requires a protein containing a region related to the GTP-binding domain of dynamin. *Genes Dev.* **6**, 380-389.

Kearns, B. G., McGee, T. P., Mayinger, P., Gedvilaite, A., Phillips, S. E., Kagiwada, S. and Bankaitis, V. A. (1997). Essential role for diacylglycerol in protein transport from the yeast Golgi complex. *Nature* **387**, 101-105.

Khvotchev, M., and Südhof, T. C. (1998). Developmentally regulated alternative splicing in a novel synaptojanin. *J. Biol. Chem.* **273**, 2306-2311.

Koenig, J. H. and Ikeda, K. (1990). Transformational process of the endosomal compartment in nephrocytes of *Drosophila melanogaster*. *Cell Tissue Res.* **262**, 233-244.

Kübler, E. and Riezman, H. (1993). Actin and fimbrin are required for the internalization step of endocytosis in yeast *EMBO J.* **12**, 2855-2862.

Lamaze, C., Fujimoto, L. M., Yin, H. L. and Schmid, S. L. (1997). The actin cytoskeleton is required for receptor-mediated endocytosis in mammalian cells. *J. Biol. Chem.* **272**, 20332-20335.

Luo, W. and Chang, A. (1997). Novel genes involved in endosomal traffic in yeast revealed by suppression of a targeting-defective plasma membrane ATPase mutant. *J. Cell Biol.* **138**, 731-746.

McPherson, P. S., Takei, K., Schmid, S. L. and De Camilli, P. (1994a). p145, a major Grb2-binding protein in brain, is co-localized with dynamin in nerve terminals where it undergoes activity-dependent dephosphorylation. *J. Biol. Chem.* **269**, 30132-30139.

McPherson, P. S., Czernik, A. J., Chilcote, T. J., Onofri, F., Benfenati, F., Greengard, P., Schlessinger, J. and De Camilli, P. (1994b). Interaction of Grb2 via its Src homology 3 domains with synaptic proteins including synapsin I. *Proc. Nat. Acad. Sci. USA* **91**, 6486-6490.

McPherson, P. S., Garcia, E. P., Slepnev, V. I., David, C., Zhang, X., Grabs, D., Sossin, W., Bauerfeind, R., Nemoto, Y. and De Camilli, P. (1996). A presynaptic inositol-5-phosphatase. *Nature* **379**, 353-357.

Micheva, K. D., Kay, B. K. and McPherson, P. S. (1997). Synaptojanin forms two separate complexes in the nerve terminal. Interactions with endophilin and amphiphysin. *J. Biol. Chem.* **272**, 27239-27245.

Mitchell, C. A., Brown, S., Campbell, J. K., Munday, A. D. and Speed, C. J. (1996). Regulation of second messengers by the inositol polyphosphate 5-phosphatases. *Biochem. Soc. Trans.* **24**, 994-1000.

Mundigl, O., Ochoa, G. C., David, C., Slepnev, V., Kabanov, A. and De Camilli, P. (1998). Amphiphysin I antisense oligonucleotides inhibit neurite outgrowth in cultured hippocampal neurons. *J. Neurosci.* **18**, 93-103.

Munn, A. L., Stevenson, B. J., Geli, I. and Riezman, H. (1995). *end5*, *end6*, and *end7*: Mutations that cause actin delocalization and block the internalization step of endocytosis in *Saccharomyces cerevisiae*. *Mol. Biol. Cell* **6**, 1721-1742.

Nemoto, Y., Arribas, M., Haffner, C. and DeCamilli, P. (1997). Synaptojanin 2, a novel synaptojanin isoform with a distinct targeting domain and expression pattern. *J. Biol. Chem.* **272**, 30817-30821.

Novick, P. and Botstein, D. (1985). Phenotypic analysis of temperature-sensitive yeast actin mutants. *Cell* **40**, 405-416.

Novick, P., Osmond, B. C. and Botstein, D. (1989). Suppressors of yeast actin mutations. *Genetics* **121**, 659-674.

Prescianotto-Baschong, C. and Riezman, H. (1998). Morphology of the yeast endocytic pathway. *Mol. Biol. Cell* **9**, 173-189.

Pringle, J. R., Preston, R. A., Adams, A. E. M., Stearns, T., Drubin, D. G., Haarer, B. K. and Jones, E. W. (1989). Fluorescence microscopy methods for yeast. *Methods Cell Biol.* **31**, 357-435.

Raths, S., Rohrer, J., Crausaz, F. and Riezman, H. (1993). *end3* and *end4*: two mutants defective in receptor-mediated and fluid-phase endocytosis in *Saccharomyces cerevisiae J. Cell Biol.* **120**, 55-65.

Rieder, S. E., Banta, L. M., Kohrer, K., McCaffery, J. M. and Emr, S. E. (1996). Multilamellar endosome-like compartment accumulates in the yeast vps28 vacuolar protein sorting mutant. *Mol. Biol. Cell* **7**, 985-999.

Riezman, H. (1985). Endocytosis in yeast: several of the yeast secretory mutants are defective in endocytosis. *Cell* **40**, 1001-1009.

Riezman, H., Munn, A., Geli, M. I. and Hicke, L. (1996). Actin-, myosin- and ubiquitin-dependent endocytosis. *Experientia* **52**, 1033-41.

Ringstad, N., Nemoto, Y. and De Camilli, P. (1997). The SH3p4/SH3p8/SH3p13 protein family: binding partners for synaptojanin and dynamin via a Grb2-like Src homology 3 domain. *Proc. Nat. Acad. Sci. USA* **94**, 8569-8574.

Sakisaka, T., Itoh, T., Miura, K. and Takenawa, T. (1997). Phosphatiylinositol 4,5-bisphosphate phosphatase regulates the arrangement of actin filaments. *Mol. Cell. Biol.* **17**, 3841-3849.

Schmalzing, G., Richter, H. P., Haansen, A., Schwarz, W., Just, I. and Aktories, K. (1995). Involvement of the GTP binding protein Rho in constitutive endocytosis in *Xenopus laevis* oocytes. *J. Cell Biol.* **130**, 1319-1332.

Shaw, J. M., Otsuga, D., Keegan, B., Hermann, G. and Bleazard, W. (1997). The dynamin-like GTPase, DNM1p, is required for maintanance of yeast mitochondrial network morphology. Abstract, ASCB meeting 1997.

Sikorski, R. S. and Hieter, P. (1989). A system of shuttle vectors and yeast host strains designed for efficient manipulation of DNA in *Saccharomyces cerevisiae*. *Genetics* **122**, 19-27.

Singer, B. and Riezman, H. (1990). Detection of an intermediate compartment involved in transport of α-factor from the plasma membrane to the vacuole in yeast *J. Cell Biol.* **110**, 1911-1922.

Singer-Krüger, B., Frank, R., Crausaz, F. and Riezman, H. (1993). Partial purification and characterization of early and late endosomes from yeast *J. Biol. Chem.* **268**, 14376-14386.

Singer-Krüger, B., Stenmark, H. and Zerial, M. (1995). Yeast Ypt51p and mammalian Rab5: counterparts with similar function in the early endocytic pathway. *J. Cell Sci.* **108**, 3509-3521.

Singer-Krüger, B. and Ferro-Novick, S. (1997). Use of a synthetic lethal screen to identify yeast mutants impaired in endocytosis, vacuolar protein sorting and the organization of the actin cytoskeleton. *Eur. J. Cell Biol.* **74**, 365-375.

Srinivasan, S., Seaman, M., Nemoto, Y., Daniell, L., Suchy, S. F., Emr, S. E., De Camilli, P. and Nussbaum, R. (1997). Disruption of three phosphatidylinositol-polyphosphate 5-phosphatase genes from *Saccharomyces cerevisiae* result in pleiotropic abnormalities of vacuole morphology, cell shape, and osmohomeostasis. *Eur. J. Cell Biol.* **74**, 350-360.

Stolz, L. E., Huynh, C. V., Thorner, J., and York, J. D. (1998). Identification and characterization of an essential family of inositol polyphosphate 5-phosphatases (*INP51*, *INP52* and *INP53* gene products) in the yeast *Saccharomyces cerevisiae*. *Genetics* **148**, 1715-1729.

Toker, A. and Cantley, L. C. (1997). Signalling through the lipid products of phosphoinositide-3-OH kinase. *Nature* **387**, 673-676.

Vida, T. A. and Emr, S. D. (1995). A new vital stain for visualizing vacuolar membrane dynamics and endocytosis in yeast. *J. Cell Biol.* **128**, 779-792.

Wendland, B., McCaffery, J. M., Xiao, Q. and Emr, S. D. (1996). A novel fluorescence-activated cell sorter-based screen for yeast endocytosis mutants identifies a yeast homologue of mammalian eps15. *J. Cell Biol.* **135**, 1-16.

Whitters, E. A., Cleves, A. E., McGee, T. P., Skinner, H. B. and Bankaitis, V. A. (1993). Sac1p is an integral membrane protein that influences the cellular requirement for phospholipid transfer protein function and inositol in yeast. *J. Cell Biol.* **122**, 79-94.

Wigge, P., Kohler, K., Vallis, Y., Doyle, C. A, Owen, D., Hunt, S. P., and McMahon, H. T. (1997). Amphiphysin heterodimers: potential role in clathrin-mediated endocytosis. *Mol. Biol. Cell* **8**, 2003-2015.

Witke, W., Podtelejnikov, A. V., Di Nardo, A., Sutherland, J. D., Gurniak, C. B., Dotti, C., and Mann, M. (1998). In mouse brain profilin I and profilin II associate with regulators of the endocytic pathway and actin assembly. *EMBO J.* **17**, 967-976.

Woscholski, R. and Parker, P. J. (1997). Inositol lipid 5-phosphatases-traffic signals and signal traffic. *Trends Biochem. Sci.* **22**, 427-431.